Vesicles with Hollow Rods in the Walls: A Trapped Intermediate Morphology in the Transition of Vesicles to Inverted Hexagonally Packed Rods in Dilute Solutions of PS-*b*-PEO

Kui Yu, Carl Bartels, and Adi Eisenberg*

Department of Chemistry, McGill University, 801 Sherbrooke Street West, Montreal, Quebec, Canada H3A 2K6

Received June 22, 1998

The preparation of block copolymer vesicles in dilute solution is well-known.[1,2] The method used in studies from this laboratory involves the dissolution of a block copolymer, such as polystyrene-*b*-poly(acrylic acid) (PS-*b*-PAA) or polystyrene-*b*-poly(ethylene oxide) (PS-*b*-PEO), in a common solvent that is good for both blocks, such as *N*,*N*-dimethylformamide (DMF), followed by the addition of water to induce the aggregation of the longer PS block. The vesicles are only one of a wide range of block copolymer morphologies that have been prepared by this method.[1] Very recently, a morphology consisting of hexagonally packed hollow hoops (HHHs) made from PS-*b*-PAA in dilute solution was identified.[3] These structures with inverted morphologies are prepared by the addition of NaCl to induce the aggregation of preformed small PS-*b*-PAA vesicles in a DMF−water mixture. As a result of the adhesion of individual primary vesicles, large compound vesicles (LCVs) form initially and subsequently rearrange to the HHH form. The PS-*b*-PAA HHHs are lined with PAA chains and are distributed in a solid PS matrix. They bear some similarity to copolymer microdomains of hexagonally packed cylinders (H) in the bulk; however, the inverted rods form hoops because the end-capping energy of the rods in the size range studied is greater than the curvature energy. Thomas et al. had also reported the effect of size on the block copolymer morphologies by isolating, for small particle sizes, concentric spherical shells, a chaotic bicontinuous structure, and a distorted network for polymers that in the bulk exhibit lamellae or a double diamond structure.[4] In the present paper, we describe a new morphology that consists of vesicles with hollow rods running inside and parallel to the surfaces of the walls. The structures are trapped intermediates in the morphological transition from vesicles to inverted hexagonally packed rods or hoops (HHRs or HHHs). The vesicles with hollow regions in the walls are referred to as "nonclassical" in the present study.

Polystyrene-*b*-poly(ethylene oxide) (PS-*b*-PEO) diblocks were synthesized by sequential anionic polymerization in tetrahydrofuran (THF), based on published procedures,[5] using cumylpotassium as the initiator; each of the diblocks gave one narrow SEC peak. The samples are denoted, for example, as PS(100)-*b*-PEO(30), showing that this particular copolymer contains 100 repeat units of styrene and 30 of ethylene oxide. In addition to this sample, the copolymers PS(125)-*b*-PEO(94) and PS(125)-*b*-PEO(30) were also prepared. To prepare the aggregates, the diblocks were stirred in tetrahydrofuran (THF) at 1 wt % for more than 4 h to get the polymer into a homogeneous single chain form. Then deionized water was added dropwise with stirring to induce self-assembly of the PS. After the water content had reached ca. 90 wt %, the solution was dialyzed against distilled water to remove the THF. An alternative way, the annealing method, involved stirring the solution overnight once a desired water content (e.g., 35 wt %) had been reached. Then more water was added gradually until the water content reached ca. 90 wt %. Again, dialysis was performed as before. After dialysis, the solution was diluted further (with ca. 10 volumes of water) and a drop was placed onto a copper EM grid, which had been precoated with a thin film of Formvar and then with carbon. The sample grid was shadowed with a palladium/platinum alloy.[1] A Phillips EM400 or 400T transmission electron microscope operating at an acceleration voltage of 80 kV was used for the morphological study.

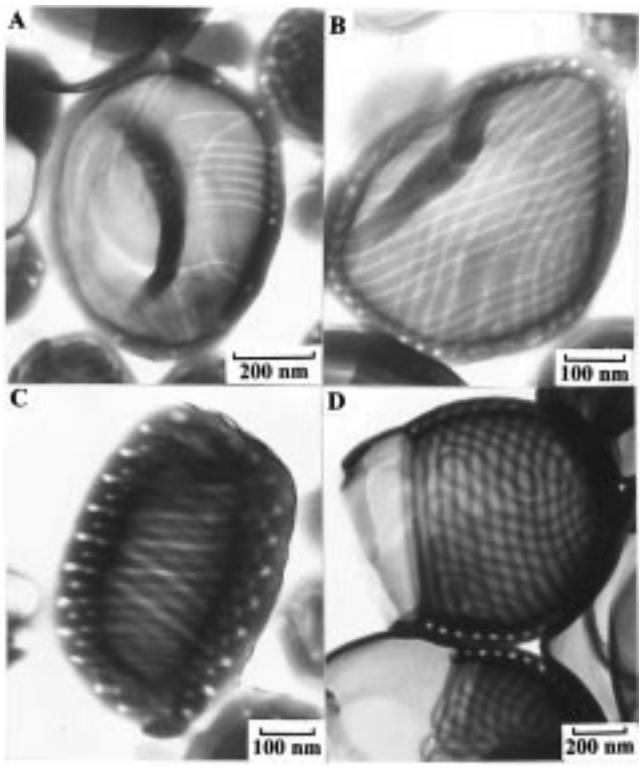

Figure 1. Vesicles with hollow regions in the walls: (A−C) the wall thickening is seen over the whole vesicle; (D) only parts of the vesicle have thickened walls.

Aggregates prepared by the annealing method from PS(100)-*b*-PEO(30) are characterized by the coexistence of several morphologies, including classical and nonclassical vesicles, as well as HHHs or HHRs. For classical vesicles, the wall thickness is very uniform and of the order of 23 ± 3 nm. The vesicle sizes are polydisperse; the outer radii (R_{out}) range from 35 to 500 nm, with the majority in the range 150−300 nm. Examples of nonclassical vesicles made from PS(100)-*b*-PEO(30) are shown in Figure 1A−C. The vesicular nature can be deduced from the increased brightness in the central parts of the aggregates compared with that on their periphery, indicating that the structures are hollow. In addition, these aggregates are three-dimensional as

* To whom correspondence should be addressed.

10.1021/ma9809785 CCC: $15.00
Published on Web 12/05/1998

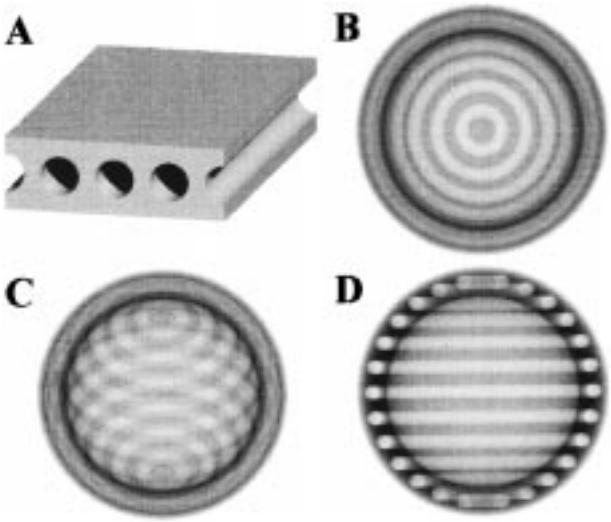

Figure 2. Computer-generated images of nonclassical bilayers with one set of hollow rods: (A) a flattened bilayer; (B−D) a nonclassical vesicle viewed from 0°, 45°, and 90° relative to the poles, respectively.

judged from the shapes of their shadowed regions. For the pictures in Figure 1A−D, the shadowed regions cannot be seen because the exposure time for printing was such as to maximize the detailed structures of the aggregates and not that of their shadowed regions. It is known that vesicles may deform from their spherical state by partly indenting, collapsing, or even breaking during the preparation of the TEM sample grids. Such indentations are seen in Figure 1A,B. These vesicles are different from the classical ones in that there are substructures in their walls, as can be seen from the nonuniform bright field image intensity in the central parts of the aggregates. The regions (in the vesicle walls) with a higher transmission indicate a lower density of the copolymer chains and appear as curved or straight lines which frequently join at the bright circular spots around the periphery of the visible edges. The wall thicknesses of the nonclassical vesicles are thicker than those of the classical ones. As measured directly from the TEM micrographs, the wall thicknesses of the nonclassical vesicles in Figure 1A,B are of the order of 45−50 nm, which is ca. twice the thickness of the classical vesicles. We suggest, therefore, that these nonclassical aggregates are vesicles with hollow rods in their thickened walls. In aqueous solution, these hollow regions are filled with both water and the PEO blocks. During the TEM sample preparation, water diffuses out, leaving them hollow. The PEO segments line the walls.

For Figure 1A−C, the wall thickening occurs over the whole vesicle; however, in some other cases, only parts of the vesicle have thickened walls, as shown in Figure 1D. This latter figure demonstrates clearly the difference in wall thickness between the classical and nonclassical parts of the vesicle. The aggregates (shown in Figure 1D) were made from a mixture of PS(125)-*b*-PEO(94) and PS(125)-*b*-PEO(30) in a weight ratio of ca. 1 to 4, which gives the composition equivalent to PS(125)-*b*-PEO(43); the method of continuous water addition was employed.

To help understand and confirm the proposed structures, i.e., vesicles with hollow regions in the walls, a computer visualization is used, as shown in Figure 2. The software used to create the images of the aggregates is POV-ray 3.02 for Linux (Persistence of Vision, TM). Figure 2A illustrates the structure of a flattened patch from a nonclassical vesicle. The figure depicts a rectangular box with parallel tubes running through it, parallel to the surface. The method of drawing this image consists of creating a solid rectangular box and subtracting the regions where the hollow rods are supposed to exist. Figure 2B−D illustrates an ideal nonclassical vesicle viewed from different angles. These images are based on the assumption that the hollow rods are simple tori which run through the wall of a vesicle. Note that, in this case, the hollow rods are all parallel to each other. The method used to create these images consists of filling the region of the vesicle wall with a fog and then removing this fog from the regions that are supposed to contain the hollow rods. The viewing angles for the different images in parts B, C, and D of Figure 2 are 0°, 45°, and 90° relative to the poles, respectively. In all cases, the size of the hollow rods, relative to the thickness of the walls, was chosen to reflect that of a typical nonclassical vesicle. It is important to note that the values of the ratio fluctuate from vesicle to vesicle and even between different locations within a vesicle.

As shown in Figure 1A−D, there are different kinds of nonclassical vesicles. This range of appearance of these vesicles is due to differences in the substructures in the vesicle walls. The hollow rods may run in the same or in different directions (but always parallel to the surfaces), as shown in Figure 1A. The formation of the hollow rods in Figure 1A is incomplete; the structure has been "frozen" before the inverted rods were fully developed. The hollow rods may be helical (Figure 1B,C); the lines appear to cross or intersect, which is due to the fact that the hollow regions of both the front and back sides of the aggregates are seen. As measured directly from the TEM micrographs, the average outer diameter of the vesicles shown in parts A and B of Figure 1 is of the order of 500 nm. In the regions of the alternating darkness and brightness, the width of the dark regions, which are thought to be "PS supports", is ca. 15−20 nm, and the diameter of the bright regions, which are thought to be the hollow rods, is ca. 5−10 nm.

Figure 1C is of particular interest, in that it shows a vesicle with a wall that has grown to a thickness of ca. 95 nm, in which the hollow rods are arranged in four sets of concentric helices (parallel to the surfaces). The regularity of the concentric helices in Figure 1C is much higher than that in Figure 1B. The very high degree of regularity in the alignment of the substructures in some of the aggregates suggests that a process similar to crystallization the hollow rods may be operative during the formation of these structures. The relative location of the hollow rods in Figure 1C is reminiscent of the H phase of block copolymers in the bulk, the PS-*b*-PAA HHH morphology, and the inverted hexagonal phase (H_{II}) of small molecule amphiphiles. The external shape of this aggregate appears barrel-shaped, approaching a cylindrical shape, with a height of ca. 600 nm and a diameter of ca. 400 nm. The hollow regions at the left periphery of the vesicle appear to be bright circular spots and at the right edge to be bright bent rods. This difference is caused by the fact that the viewing direction is not perpendicular to the main axis of the helices, i.e., the main axis of the cylinder. A similar effect can be observed when viewing a helical spring from a direction slightly away from the normal to the main

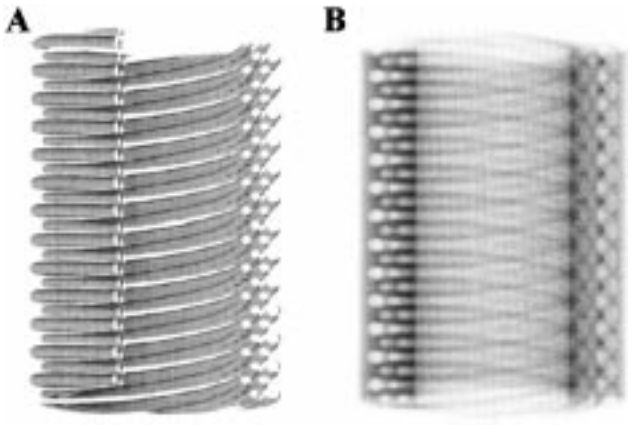

Figure 3. Computer-generated image of a nonclassical cylinder with four sets of hollow helices: (A) an image of the hollow helices alone with a 110° cut; (B) an image obtained by confining the transparent hexagonally packed hollow helices into a semitransparent hollow cylindrical copolymer matrix. The view direction is 10° away from the normal to the major axis of the cylinder.

axis. The average diameter of the hollow spots is ca. 5−15 nm. The center-to-center distance of the two neighboring hollow spots in one set parallel to the surface is ca. 65 nm, and that of two nearest neighbors is ca. 35 nm.

Again, a computer visualization is used to depict the structure of the wall shown in Figure 1C. The spiral morphology was reproduced on a computer by making a cylindrical wall of fog and removing the helical portions from this, as shown in Figure 3. The image attempts to depict, as closely as possible, the details of Figure 1C which it represents. To do this, a set of 12 hollow helices was designed to be coiled together so that the resulting helix contained four close-packed layers where each layer had three interweaving hollow helices. This was done to reflect the same features seen in Figure 1C. The diameter of the outermost hollow spiral was made 20% larger than those of inner ones. This value of the increase in diameter (for the outermost layer) only refers to the specific vesicle shown in Figure 1C and is not a general phenomenon. While the representation is not exact, we believe that it does contain all the essential features of the morphology.

The image in Figure 1D shows both the hollow regions and the PS "supports" of the front and back sides. The degree of regularity of the regions of alternating light and dark lines is high. Especially, the uniformity of the width of the dark lines (i.e., PS "supports") is worthy of notice. As measured, the width of the PS "supports" and the average wall thickness of the original classical bilayers are the same, i.e., ca. 20 nm. In addition, the average wall thickness of the nonclassical sections is ca. 70 nm. The upper edge of the upper vesicle is seen to be slightly wavy, with the crests located above the hollow spots.

It seems reasonable to suggest that the nonclassical vesicles described here are trapped intermediates in the morphological transition from vesicles to inverted hexagonally packed hoops or rods (HHHs or HHRs). The nonclassical vesicles can have a very different appearance, but they have in common both the vesicular nature and the presence of hollow regions in the wall. When there are more than one set of hollow rods, these hollow rods tend to arrange themselves in a hexagonal array. Thus, it appears that the vesicles with hollow regions in the wall form in the initial stage of the transition. The average diameter of the inverted rods and the average center-to-center distance between two nearest-neighbor rods change in the course of the transition.

Thus, the mechanism of the transition from PS-*b*-PEO vesicles to HHHs or HHRs involves thickening of the vesicle walls and the formation of hollow rods in the wall running parallel to the surfaces, accompanied by a decrease of the size of the hollow vesicular core. This mechanism does not involve fusion of preformed vesicles in the early stages and is thus different from that found either for small molecule amphilphiles or for PS-*b*-PAA diblocks.[3,6] When large unilamellar vesicles of small molecule amphiphiles are subjected to conditions under which the transition from lamellae (L_α) to inverted hexagonally packed cylinder phases (H_{II}) occurs, intervesicular mixing and fusion are observed. Thus, the formation of the H_{II} phases involves fusion of large unilamellar vesicles.[6] As mentioned before, the formation of one PS-*b*-PAA HHH aggregate also involves aggregation of many small vesicles upon the addition of salt.[2] The reason for the different mechanisms of the transition may be due to the strength of the inter corona or headgroup repulsion of the precursor vesicles. The PEO repulsion is relatively weak, while for the ionizable PAA or the charged headgroups (of small molecule amphiphiles), the repulsions are relatively strong. Each individual vesicle is stabilized, i.e., vesicle fusion is avoided, due to the electrostatic and/or steric repulsion. The addition of salt (to PS-*b*-PAA vesicles) and the change of pH (for lipid veislces) decrease the strong electrostatic repulsion so that these vesicles can fuse with each other. This aspect will be explored in a future paper.[7]

It is necessary to point out that the morphological transition in PS-*b*-PAA from vesicles to inverted rods with a hexagonal array was driven by added salt (NaCl). For the present system, the transition is caused by an increase in the water concentration, which accomplishes the same function as the addition of the salt to the PS-*b*-PAA small vesicles; i.e., it drives the morphology from a bilayer to the next stage, i.e., inverted hexagonally packed rods. During the transition, the intermediates, i.e., vesicles with hollow regions in the wall, are trapped. THF appears to be particularly useful in trapping intermediate morphologies, because the range of water contents in which the kinetics are relatively slow but still finite is much wider than that in DMF. Thus, a higher degree of control can be exercised over the relevant kinetics. Of course, further study of the detailed kinetics is necessary.

The L_α/H_{II} transition has generated intense interest; one of the reasons for the high level of interest is that the initial intermediates of the L_α/H_{II} transition are believed to be the same as those of biomembrane fusion.[6] The intermediates of the later stages of the present transition are found to be similar to those of lipid vesicles after fusion. This aspect will be discussed in a forthcoming paper.[7] Thus, the present study may shed some light on the process of biomembrane fusion and the lipid lamella (L_α) to inverted hexagonal (H_{II}) phase transition. It is noteworthy that biomembrane thickening was reported recently,[8] although the study did not deal with the L_α/H_{II} transition, and the mechanism was thus very different.

In conclusion, self-assembled vesicles with hollow rods running parallel to the surfaces of the walls have been prepared from PS-*b*-PEO diblocks in dilute solution. Such structures are trapped intermediates in the morphological transition from vesicles to inverted aggregates of HHHs or HHRs. The formation of these nonclassical vesicles involves thickening of vesicle walls accompanied by the formation of the hollow rods in the wall and a decrease of the sizes of the hollow cores. The present observation of nonclassical vesicles suggests that the mechanism of the transition from vesicles to inverted hexagonally packed rods or hoops is different from those found in PS-*b*-PAA and in small molecule amphiphile systems.

Acknowledgment. We thank The Natural Science and Engineering Research Council of Canada (NSERC) for financial support of this research. We are indebted to Dr. J. K. Cox for useful discussions.

References and Notes

(1) (a) Zhang, L.; Eisenberg, A. *Science* **1995**, *268*, 1728. (b) Zhang, L.; Yu, K.; Eisenberg, A. *Science* **1996**, *272*, 1777. (c) Yu, K.; Eisenberg, A. *Macromolecules* **1996**, *29*, 6359. (d) Yu, K.; Zhang, L.; Eisenberg, A. *Langmuir* **1996**, *12*, 5980. (e) Yu, Y.; Eisenberg, A. *J. Am. Chem. Soc.* **1997**, *119*, 8383. (f) Yu, K.; Eisenberg, A. *Macromolecules* **1998**, *31*, 3509. (g) Zhang, L.; Eisenberg, A. *Polym. Adv. Technol.* **1998**, *9*, 677.

(2) (a) Ding, J.; Liu, G. *Macromolecules* **1997**, *30*, 655. (b) Iyama, K.; Nose, T. *Polymer* **1998**, *39*, 651.

(3) Zhang, L.; Bartels, C. Yu, Y.; Shen, H.; Eisenberg, A. *Phys. Rev. Lett.* **1997**, *79*, 5034.

(4) Thomas, E. L.; Reffner, J. R.; Bellare, J. *Colloq. Phys.* **1990**, *51* (23), C7, 363.

(5) (a) Ziegler, K.; Dislich, H. *Chem. Ber.* **1957**, *90*, 1107. (b) O'Malley, J. J.; Marchessault, R. H. *Macromol. Synth.* **1972**, *4*, 35. (c) Hruska, Z.; Hurtrez, G.; Walter, S.; Riess, G. *Polymer* **1992**, *33*, 2447.

(6) (a) Chu, C. J.; Szoka, F. C., Jr. *J. Liposome Res.* **1994**, *4* (1), 361. (b) Seddon, J. M. *Ber. Bunsen-Ges. Phys. Chem.* **1996**, *3*, 380. (c) Siegel, D. P.; Epand, R. M. *Biophys. J.* **1997**, *73*, 3089.

(7) Yu, K.; Bartels, C.; Eisenberg, A. Manuscript in preparation.

(8) Schmidtgen, M. C.; Drechsler, M.; Lasch, J.; Schubert, R. *J. Microsc.* **1998**, *191*, 177.

MA9809785